CHEMISTRY
A EUROPEAN JOURNAL

DOI: 10.1002/chem.201000541

2-Hydroxyazobenzenes to Tailor pH Pulses and Oscillations with Light

Matthieu Emond,[a] Thomas Le Saux,[a] Sylvie Maurin,[a] Jean-Bernard Baudin,[a] Raphael Plasson,[b] and Ludovic Jullien*[a]

Abstract: This paper evaluates the 2-hydroxyazobenzene platform for tailoring proton concentration pulses and oscillations with monochromatic light. The easily prepared 2-hydroxyazobenzenes exhibit large absorptions in the near-UV range. Photoisomerization was investigated by UV/Vis absorption, ^{1}H NMR spectroscopy, and steady-state fluorescence emission. In the whole investigated series, the *trans* stereoisomer of the 2-hydroxyazobenzene motif provides the corresponding *cis* derivative with an action cross section in the $10^3\,\text{M}^{-1}\,\text{cm}^{-1}$ range. At the same time, photoisomerization is accompanied by a significant pK drop of the phenol group. According to the phenyl-substituent pattern, *cis*-to-*trans* thermal back-isomerization can be tuned in the 10 ms–100 s range. Up to 2 units of reversible pH drops or pH oscillations on the 10 s timescale have been obtained by appropriately tailoring single-wavelength illumination of 2-hydroxyazobenzene solutions.

Keywords: acidity · azo compounds · isomerization · photochromism · protonation

Introduction

The proton is the essential ion that rules exchanges between acidic and basic groups.[1] Its reaction with a molecule often leads to major alterations of structure and reactivity, which makes it a ubiquitous catalyst.[2] The investigation of the role of the proton on the behavior of reactive systems is well established in chemistry as well as in biology. However, whereas buffers are traditionally used to investigate thermodynamic aspects of proton significance,[3] specific tools have to be developed to interrogate kinetic aspects that require to control the temporal variation of the proton concentration.

Photochemistry is particularly attractive here, as it can provide a noninvasive road with spatial and temporal resolution. Proton photoactivation can rely on a photoacid, which irreversibly photoreleases a proton once illuminated. This situation is encountered in caged weak bases such as phosphates[4] and sulfates,[5] or in *o*-nitrobenzaldehydes that yield a benzoic acid after photorearrangement.[6–8] Alternatively, the proton may be only transiently photoreleased from a photoacid, thereby making it possible to shape proton pulses with light.[9] In particular, this feature opens a road to extract rate constants and mechanisms of processes that involve protons by analyzing the dependence of the system response on the frequency of periodic oscillations of proton concentration.[10,11] Interestingly, since proton exchanges are fast[1] and often interfere with various chemical reactions, reversible photoacids could also be used to investigate, along the same way, the kinetics and mechanisms of other processes that involve inorganic ions,[12] biomolecules,[13,14] or synthetic systems.[15]

In relation to molecular engineering, three parameters are relevant to photogenerate periodic pH oscillations (see the Supporting Information): 1) the shift of the proton-exchange thermodynamic constant upon photoactivation of the rever-

[a] M. Emond, Dr. T. Le Saux, S. Maurin, Prof. Dr. J.-B. Baudin, Prof. Dr. L. Jullien
Ecole Normale Supérieure, Département de Chimie
UMR CNRS-ENS-UPMC Paris 06 8640 Pasteur
24, rue Lhomond, 75231 Paris Cedex 05 (France)
Fax: (+33) 1-4432-3325
E-mail: Ludovic.Jullien@ens.fr

[b] Dr. R. Plasson
Nordita, Roslagstullsbacken 23, 10691 Stockholm (Sweden)

Supporting information for this article is available on the WWW under http://dx.doi.org/10.1002/chem.201000541. It contains a simple model to analyze the pH change resulting from illuminating a reversible photoacid; the organic syntheses; the derivation of the proton-exchange constants of the *trans* stereoisomers of the 2-hydroxyazobenzenes (Figure 1S); the evidence for the *trans*-to-*cis* photochemical isomerization of TH_2Cl_3 (Figures 2S and 3S); the kinetic analysis of the photochemical behavior of 2-hydroxyazobenzenes: theory and experimental results (Figures 4S–8S); the protocol for correcting the emission from the fluorescent pH reporter from the variation of the sample absorbance (Figures 9S–12S); and the numerical simulation protocol for proton concentration pulses (Figure 13S).

sible photoacid AH ($pK_{AH*}-pK_{AH}$); 2) the ratio of the average concentrations in the photoactivated and in the ground states (AH*/AH); and 3) the relaxation time associated with the deactivation of the AH* photoactivated state. Together with the total photoacid concentration, the two first parameters control the maximal amplitude of the pH oscillation which can be obtained from periodically modulating the illumination of the photoacid, whereas the third parameter controls the effective amplitude which can be reached at a given light modulation frequency. To get pH oscillations of significant amplitude in a broad range of light modulation frequencies, one has to favor a photoacid that exhibits a large $pK_{AH*}-pK_{AH}$ shift and a high rate of relaxation of the photoactivated state, and to increase light intensity to reach a large AH*/AH ratio.

From the first point, molecules such as phenols that exhibit a p*K* value of their first electronic excited state that is up to ten units lower than the p*K* of their ground state could seem particularly attractive.[16,17] Indeed, they have been fruitfully used to photogenerate transient out-of-equilibrium states to investigate local buffering properties of various media. However, the short lifetime of singlet excited states is a major limitation to the generation of significant overall acidifications: powerful light sources would have to be used with the risk of encountering detrimental side effects. In fact, the delivery of significant pH pulses requires the lifetime of the photoactivated state AH* to be longer-lived than an electronic excited state but still short-lived enough to get a good temporal resolution.

Photocontrolled reorganization of the conjugated pathway between donor- and acceptor-terminating groups that bear acidic or basic functions is here a first strategy.[18–20] However, the illumination of the already investigated molecules led only to modest changes of p*K*. Photoisomerization of substituted aromatic rings that transiently generate acidic groups has also been examined,[21–23] although not explicitly in relation to the photocontrol of proton-exchange thermodynamic constants. Provided the reported photochemical behavior is robust enough,[24] this approach could be attractive. The alteration of the environment of an acidic group after photoisomerization could also be used to generate proton pulses with light. The corresponding alteration generally provides only modest changes of proton-exchange constants.[25–27] In contrast, from partition coefficient measurements, Haberfield derived promising orders of magnitude for the photoenhancement of the ionization constants of two 2-hydroxyazobenzenes.[28] The best observed factor of 600 was explained by environmental changes of the acidic proton upon illumination: in the *trans* stereoisomer, acidity is diminished by the hydrogen bond between the phenol and an azo nitrogen, whereas in the *cis* configuration, the hydrogen bond is lost and the intrinsic acidity of the substituted phenol is restored (see Scheme 2; see below).[29] However, Haberfield's purpose of investigating photocontrolled phase transfer made it impossible to get any insight about the lifetime of the photoactivated acidic *cis* stereoisomer, thus preventing the evaluation of the relevance of the system toward the photogeneration of pH pulses or oscillations.

Considering the last-mentioned results as well as the explanation that accounts for the photoinduced acidity, we have envisioned that the 2-hydroxyazobenzene backbone could provide a versatile platform for building a series of reversible photoacids appropriate for tailoring significant pH pulses and oscillations. Numerous synthons are commercially available to achieve efficient syntheses of 2-hydroxyazobenzenes in one step. Changing starting materials should provide an easy way to alter solubility of the targeted 2-hydroxyazobenzenes as well as both their photophysical and acidic properties in the ground and photoactivated states. Structural changes should be similarly expected to provide a road to finely tune the kinetics for thermal return from the photoactivated *cis* stereoisomer, which is known to be faster than the corresponding azobenzene series.[29–31] Azobenzenes are additionally well known for the robustness of their photochromism:[32,33] 2-hydroxyazobenzenes should exhibit no significant fatigue upon multiple photocycles that lead to proton pulses. Eventually, their ionization that accompanies proton photorelease during the *trans*-to-*cis* photoisomerization could further enlarge the broad field of relevance of the azobenzene moiety, which has been extensively used to photocontrol the behavior of small molecules as well as of natural and synthetic macromolecules.[34]

The present paper examines the 2-hydroxyazobenzene platform in the generation of light-driven pH pulses and oscillations. The first section deals with the design and the syntheses of two series of 2-hydroxyazobenzene derivatives that differ by the substitution pattern of the phenyl rings borne by the nitrogen–nitrogen double bond. The second section investigates the acid–base, photophysical, and photochemical properties of those 2-hydroxyazobenzenes. The third section implements two 2-hydroxyazobenzenes in the photogeneration of pulses and oscillations of proton concentration.

Abstract in French: *Cet article étudie la plateforme 2-hydroxy-azobenzène afin d'obtenir des sauts ou des oscillations de concentration de proton sous irradiation monochromatique. Les 2-hydroxy-azobenzènes sont facilement synthétisés et présentent une bande d'absorption intense dans le proche UV. La photoisomérisation de ces molécules a été étudiée par spectroscopie UV-Visible, RMN ^1H et par fluorimétrie. Dans toute la série, l'isomère trans est transformé en isomère cis avec une section efficace de photoconversion de l'ordre $10^3\,M^{-1}\,cm^{-1}$. Cette photoisomérisation s'accompagne d'une diminution significative du p*K*a du groupe phénol. Suivant la nature du substituant en para du noyau aniline, l'isomérisation thermique* cis/trans *peut se produire à une échelle de temps caractéristique comprise entre 10 ms et 100 s. Des sauts de pH de presque deux unités et des oscillations à une période de l'ordre de la dizaine de secondes ont été observés en illuminant convenablement des solutions de 2-hydroxyazobenzène à une seule longueur d'onde.*

Results and Discussion

Design and synthesis: In the present study, we were willing to evaluate the robustness of the change of the proton-exchange thermodynamic constant as a function of the molecular structure by altering the substituent pattern of the two phenyl rings of the 2-hydroxyazobenzene motif. Thus we generated two series of derivatives (Scheme 1): 1) starting from the most promising compound investigated by Haberfield,[28] we retained 2,4,5-trichlorophenol for the phenol moiety in the first series: $THRCl_3$ (R = NO_2, SO_3K, Br, COOH, H, SMe, Et, Me, OMe). In contrast, we changed the substituent borne at the *para* position of the other phenyl ring with the expectation of affecting both the strength of the hydrogen bond in the *trans* stereoisomer and the rate constant for the thermal *cis*-to-*trans* isomerization. 2) In the second series, we explored three other phenols (2,4-difluoro-, 2,4-dichloro-, and 4-nitrophenol) that bear electron-withdrawing groups,[28] and which have in common the absence of a substituent in the 6-position of the resulting 2-hydroxyazobenzenes.

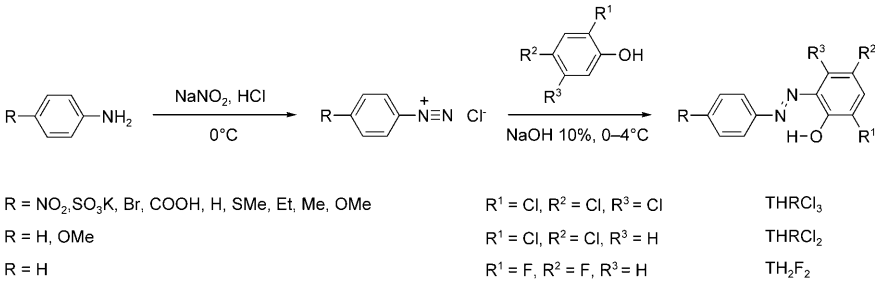

Scheme 1. Synthesis and structures of the 2-hydroxyazobenzene derivatives investigated in the present account.

The investigated 2-hydroxyazobenzene derivatives have been obtained in one step with good yields (50–80%) from coupling the appropriate phenol in a basic medium with the diazonium that results from treating the parent aniline with an excess amount of acidic solution of sodium nitrite (Scheme 1).[35–38]

Physicochemical properties

TH proton-exchange thermodynamic constants: We first examined the acid–base properties of the *trans* stereoisomers TH of the present 2-hydroxyazobenzenes. To avoid any problem of solubility in the whole series, water/acetonitrile 1:1 (v/v) was used as a solvent. The absorption spectrum of the TH derivatives was recorded as a function of the proton concentration in Britton–Robinson buffer[39] (acetic acid, boric acid, phosphoric acid; 0.04 M)/acetonitrile 1:1 (v/v). All the solutions were protected from sunlight to avoid any *trans*-to-*cis* photoisomerization (see below).

Figure 1S in the Supporting Information displays representative results obtained with TH_2Cl_3. In line with the increase of conjugation that accompanies the deprotonation of the phenol group, the absorption spectrum is redshifted in basic media ($\lambda_{max}(TH_2Cl_3) = 347$ nm at pH 7.2, whereas $\lambda_{max}(THCl_3) = 435$ nm at pH 11.1). From the whole collection of absorption spectra, we extracted $pK_{TH_2Cl_3} = 9.4$. Despite the presence of the additional -N=N- electroattractive group in the *ortho* position of the phenol moiety, this value is significantly larger than the $pK = 8.3$ that we measured for the parent 2,4,5-trichlorophenol in the same solvent. Such a large pK shift probably originates from a hydrogen bond between the proton of the phenol group and one nitrogen atom of the azo motif (see Scheme 2). This explanation is also supported by the observation that the chemical shift in the ^1H NMR spectrum of the proton borne by the hydroxy group in TH_2Cl_3 ($\delta = 14.6$ ppm) is much larger than the one observed in the parent 2,4,5-trichlorophenol ($\delta = 5.5$ ppm) in deuterated chloroform.

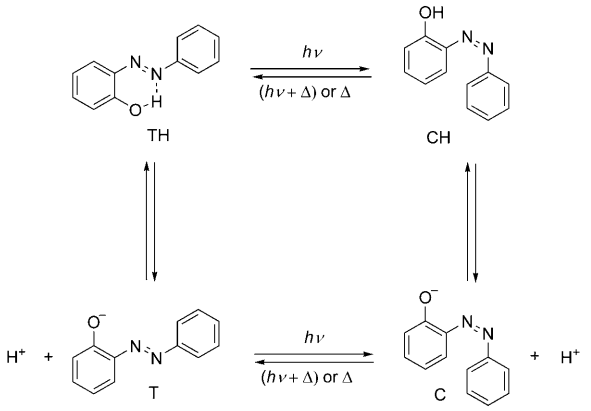

Scheme 2. Mechanism accounting for the photochemical behavior of 2-hydroxyazobenzenes.

The latter interpretation was strengthened after reproducing the same experiment in the whole $THRCl_3$ series (see Table 1). The $\lambda_{max}(THRCl_3)$, $\lambda_{max}(TRCl_3)$, and pK_{THRCl_3} values range between 347 and 416 nm, 426 and 494 nm, and 8.3 and 9.7, respectively. In particular, when the R substituent exhibits more and more electron-withdrawing properties, pK_{THRCl_3} decreases. This trend was further quantified by plotting pK_{THRCl_3} as a function of the Hammett coefficient σ_R of the R substituent.[40–42] As shown in Figure 1a, the dependence of pK_{THRCl_3} on σ_R is fairly linear. The negative slope observed for pK_{THRCl_3} is in line with a weakening of the electron density at the nitrogen site involved in the hydrogen bond in $THRCl_3$ when R becomes more and more electron withdrawing.[43]

Table 1. Maximal wavelengths of absorption and molar absorption coefficients for the acidic (λ^{TH}_{max}, $\varepsilon(\lambda^{TH}_{max})$) and basic ($\lambda^{T}_{max}$, $\varepsilon(\lambda^{T}_{max})$) states, proton-exchange constants for the *trans* (pK_{TH}) and the *cis* (pK_{CH}) stereoisomers, rate constants $k^{\Delta}_{CH\rightarrow TH}$ and $k^{\Delta}_{C\rightarrow T}$ associated with thermal *cis*-to-*trans* isomerization of the acidic CH and basic C states for the investigated 2-hydroxyazobenzenes. Solvent: Britton–Robinson buffer[39] (acetic acid, boric acid, phosphoric acid; 0.04 M)/acetonitrile 1:1 (v/v), $T = 298$ K.

TH	λ^{TH}_{max} [nm] ($\varepsilon(\lambda^{TH}_{max})$ [$mM^{-1}cm^{-1}$])	λ^{T}_{max} [nm] ($\varepsilon(\lambda^{T}_{max})$ [$mM^{-1}cm^{-1}$])	$pK_{TH} \pm 0.1$	$pK_{CH} \pm 0.1$	$k^{\Delta}_{CH\rightarrow TH} \pm 0.1$ [min^{-1}]	$10^2 \times k^{\Delta}_{C\rightarrow T}$ [min^{-1}]
$THOMeCl_3$	380 (20)	426 (4)	9.5	7.0	0.4	(3 ± 3)[a]
$THMeCl_3$	355 (22)	430 (5)	9.7	6.6	1.3	(2 ± 2)[a]
$THEtCl_3$	357 (19)	431 (4)	9.6	6.8	1.5	(2 ± 2)[a]
$THSMeCl_3$	416 (8)	441 (5)	9.6	6.7	2.6	(2 ± 2)[a]
TH_2Cl_3	347 (20)	435 (5)	9.4	6.6	4.5	<2
$THCOOHCl_3$	353 (16)	449 (5)	9.2	_[b]	_[b]	_[b]
$THBrCl_3$	355 (12)	443 (4)	8.9	_[b]	_[b]	_[b]
$THSO_3KCl_3$	349 (22)	451 (6)	8.9	_[b]	_[b]	_[b]
$THNO_2Cl_3$	354 (22)	494 (10)	8.3	_[b]	_[b]	_[b]
$THOMeCl_2$	361 (22)	475 (13)	9.2	_[b]	_[b]	_[b]
TH_2Cl_2	328 (20)	477 (10)	8.7	_[b]	_[b]	_[b]
TH_2F_2	324 (17)	470 (5)	8.8	_[b]	_[b]	_[b]

[a] From the fit with Equation (44) in the Supporting Information. [b] Thermal *cis*-to-*trans* isomerization took place too rapidly to be measured with our protocol.

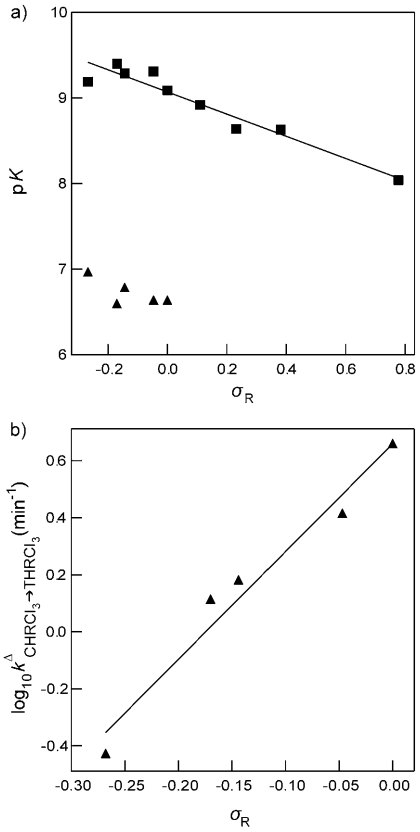

Figure 1. a) Plot of pK_{THRCl_3} (squares) and pK_{CHRCl_3} (triangles), and b) $\log_{10} k^{\Delta}_{CHRCl_3\rightarrow THRCl_3}$ as a function of the Hammett coefficient σ_R of the R substituent. Markers: experimental data; solid line: linear fit. We found: $pK_{THRCl_3} = 9.4 - 1.3\sigma_R$, $\log_{10} k^{\Delta}_{CHRCl_3\rightarrow THRCl_3}$ [min^{-1}] $= 0.66 + 3.76\sigma_R$.

The experiments performed in the second series of 2-hydroxyazobenzenes brought additional information to the preceding picture (Table 1). As in the first series, the observation $pK_{THOMeCl_2} > pK_{TH_2Cl_2}$ supports the presence of a hydrogen bond between the hydroxyl group of the phenol and a nitrogen atom. However, in contrast with the previous observations, the p*K* values of $THOMeCl_2$ (9.2), TH_2Cl_2 (8.7), and TH_2F_2 (8.8) were significantly smaller than the ones of the parent 2,4-dichlorophenol (9.4) and 2,4-difluorophenol (10.1). This behavior could be explained by a better phenol conjugation with the electron-withdrawing diazo double bond in the second series of 2-hydroxyazobenzenes, which lacks the chloro substituent at the 5-phenol position. This explanation would be supported by the trend observed in UV/Vis absorption (Table 1): for a same phenyl substituent, the removal of the 5-chloro substituent significantly redshifts the maximal wavelength of absorption of the phenolate T, in line with a larger conjugation pathway in the second series of 2-hydroxyazobenzenes.

Preliminary photochemical observation: In a series of preliminary experiments performed at 277 K (to avoid the thermal *cis*-to-*trans* isomerization; see below), we illuminated 42 μM solutions of TH_2Cl_3 in Britton–Robinson buffer[39] (acetic acid, boric acid, phosphoric acid; 0.04 M)/acetonitrile 1:1 (v/v) at 365 nm for 5 min. We subsequently recorded and compared their UV/Vis absorption spectra either immediately or ten minutes after turning off the UV light.

At pH 8.0 as well as pH 11.8 (at which points TH_2Cl_3 exists as its acidic and basic states, respectively), UV illumination caused a significant hypochromic effect (by about 50%) without major alteration of the absorption bands (Figures 2Sa and b in the Supporting Information). These observations were in line with a *trans*-to-*cis* photoisomerization both for the acidic and basic states of TH_2Cl_3. Indeed, they agreed with reported literature on 2-hydroxyazobenzenes in which the marked difference of light absorption between the *trans* and *cis* stereoisomers was interpreted as resulting from the nonplanar configuration of the *cis* isomer.[29,44] The preceding conclusions were also supported by ^{1}H NMR spectroscopic observations that showed that UV illumination of the *trans* stereoisomer generated the formation of a new species with NMR spectroscopic peaks in line with the corresponding *cis* derivative (Figure 3S in the Supporting Information). We additionally noticed that the absorption spectrum of the illuminated solution at the lowest pH fully recovered when the solution was left unilluminated for ten minutes at room temperature. In contrast, the illuminated sample at the largest pH did not exhibit any significant evolution after the same delay. We interpreted this behavior as resulting from a thermal *cis*-to-*trans* isomerization; it oc-

curred rather fast for the acidic TH_2Cl_3 state but much slower for the basic $THCl_3$ form.[29]

After the series of preliminary experiments, we adopted the mechanism shown in Scheme 2 to account for the photochemical behavior of 2-hydroxyazobenzenes: we consider the interconversion between four states: TH, T, CH, and C, which correspond to the acidic and basic conjugates of the *trans* and *cis* stereoisomers, respectively. The *trans*-to-*cis* conversion is considered to be driven by light only in view of the larger thermodynamic stability of the *trans* stereoisomer, whereas *cis*-to-*trans* isomerization can be thermally as well as photochemically driven. In contrast, proton exchanges occur under thermal control only.

CH proton-exchange thermodynamic constants: *cis*-Azobenzene stereoisomers often live long enough to be purified by chromatography.[32,45] In the present 2-hydroxyazobenzene series, the fast *cis*-to-*trans* thermal isomerization forbids both the purification and the application of the titration protocol at equilibrium to measure the CH proton-exchange thermodynamic constants. In contrast, the analysis at different proton concentrations of the kinetics of thermally driven *cis*-to-*trans* isomerization gives access to the sought-after thermodynamic constants (see Figure 4S in the Supporting Information).

We illuminated TH solutions at their wavelength of maximal absorption at various proton concentrations to photogenerate the *cis* stereoisomer CH. We subsequently analyzed in the dark the temporal relaxation of the solution absorbance to derive pK_{CH}. Table 1 displays the results for the 2-hydroxyazobenzenes for which the lifetime of the *cis* stereoisomer was large enough to apply the present protocol. The measured pK_{CH} range between 6.6 and 7.0, much below the 8.3 one obtained for the 2,4,5-trichlorophenol in Britton–Robinson buffer[39] (acetic acid, boric acid, phosphoric acid; 0.04 M)/acetonitrile 1:1 (v/v) (but close to its value in water, $pK = 6.9$[46]). Since *cis*-2-hydroxyazobenzenes cannot form the hydrogen bond present in the *trans* stereoisomers, the latter observation is significant for the evaluation of the relative contributions of the factors that govern the acidity of the 2-hydroxyazobenzenes in the TH_2Cl_3 series: The 1.0–1.5-unit pK decrease of CH with regard to the parent phenol probably evaluates the electron-withdrawing effect of the diazo double bond, whereas the 2.5-unit ($pK_{TH} - pK_{CH}$) difference reflects the strength of the hydrogen bond.

Kinetics of thermal cis-*to*-trans *isomerization*: With our instrumental setup, we were able to measure the relaxation time associated with the thermal CH *cis*-to-*trans* isomerization when it was higher than a few seconds.

In the TH_2Cl_3 series, the associated rate constants were shown to strongly depend on the proton concentration with half-times ranging between minutes (under acidic conditions) and beyond several hours (at the lowest proton concentrations). The analysis of this dependence yielded the rate constants $k^{\Delta}_{CH\rightarrow TH}$ and $k^{\Delta}_{C\rightarrow T}$ associated with thermal *cis*-to-*trans* isomerization of the acidic CH and basic C states, respectively (see Figure 4S in the Supporting Information). As shown in Table 1, whereas our experimental conditions were adapted to measure $k^{\Delta}_{CH\rightarrow TH}$ with good precision, $k^{\Delta}_{C\rightarrow T}$ was too low to be reliably evaluated. The value of $k^{\Delta}_{CH\rightarrow TH}$ strongly depends on the phenyl substituent R. The slowest thermal *cis*-to-*trans* relaxations are observed for the substituents that exhibit the strongest electron-donating properties. The corresponding free-energy linear relationship with the Hammett parameters is displayed in Figure 1b. By extending the observed linear dependence to the whole series, this study suggests that changing the $THRCl_3$ phenyl substituent is an efficient way to tune the relaxation time associated with the thermal *cis*-to-*trans* isomerization over five orders of magnitude: the 100 s range is observed with the slowest $CHOMeCl_3$, whereas 10 ms can be extrapolated for the most reactive $CHNO_2Cl_3$.

We were unable to reliably collect the rate constants associated with the thermal *cis*-to-*trans* isomerization in the second series of 2-hydroxyazobenzenes: even at the highest pH, thermal return of the photogenerated CH is already fast. For instance, it occurs in 7 min in the basic state of $CHCl_2$, whereas we did not observe any relaxation beyond the hour timescale for $CHCl_3$. In particular, the latter observation may suggest conjugation between the phenol and the diazo bond to be significant along the way from the *cis* to the *trans* stereoisomer since the second series lacks a 5-phenol substituent. The phenyl-substituent effect observed in the first series was again present: at pH 10.4, the respective relaxation times of $CHOMeCl_2$ and CH_2Cl_2 were 40 and 4 s. In addition, 2,4-difluorophenol yielded a faster thermal return than 2,4-dichlorophenol: at pH 11.7, we found 420 and 10 s for the relaxation times of CH_2Cl_2 and CH_2F_2, respectively.

The present analysis of the kinetics of thermal *cis*-to-*trans* isomerization shows that relaxation times are noticeably lower than the ones of the corresponding azobenzenes, thus making the 2-hydroxyazobenzene backbone an attractive photochromic platform for "fast" applications. In particular, photoswitching proton-exchange constants will not require two-color illumination to be kinetically efficient.

Kinetics of the photochemically driven trans-*to*-cis *and* cis-*to*-trans *isomerization*: The rate constants associated with azobenzene photochemical reactions have been often measured by recording the sample absorbance after illumination for various times.[32,45] In contrast, the present 2-hydroxyazobenzene series exhibits a thermal *cis*-to-*trans* isomerization that is too rapid to apply the same protocol. We recently implemented a protocol relying on continuous illumination to face a similar situation that involved fast photochemical events.[47–49] Here we also adopted continuous illumination and a fluorescent probe both to generate the photochemical reactions and to report on their extent by the inner filter effect. After a series of preliminary experiments (see Figures 5S and 6S in the Supporting Information), we adopted the strongly fluorescent rhodamine B probe, which is soluble

in acetonitrile/water 1:1 (v/v); it weakly absorbs in and strongly emits beyond the absorption wavelength range of TH/CH (to report on TH/CH absorbance and to avoid any absorption of the fluorescence emission by TH/CH; see Figures 2Sa and b in the Supporting Information). Moreover, rhodamine B is not sensitive to pH in the investigated range (to identically report on sample absorbance whatever the pH change during the evolution). Thus we submitted mixtures that initially contained the *trans* stereoisomer TH (typically at 5 μM concentration) and 1 μM rhodamine B to continuous illuminations while recording the intensity of the rhodamine B fluorescence emission. As expected from the formation of the less-absorbing *cis* stereoisomer, which leads to an increase in the light intensity experienced by the rhodamine B, the fluorescence intensity increases as a function of time (see Figure 7Sa in the Supporting Information). After a typical delay of a few seconds to a few tens of seconds, it subsequently reaches a plateau associated with the photosteady state. We satisfactorily fit the corresponding evolution to extract functions of the rate constants associated with the *trans*-to-*cis* and *cis*-to-*trans* isomerization for a particular light intensity at a given pH. Reproducing this experiment for various light intensities and at various proton concentrations eventually provides access to the photochemical features of the acidic and basic states at a given excitation wavelength, $\varepsilon_{TH}\Phi_{TH\rightarrow CH}$ and $\varepsilon_{CH}\Phi_{CH\rightarrow TH}$, and $\varepsilon_{T}\Phi_{T\rightarrow C}$ and $\varepsilon_{C}\Phi_{C\rightarrow T}$, in which ε and Φ refer to molar absorption coefficients and quantum yields associated with the photoisomerization (see the Supporting Information). As ε_{TH} and ε_{T} can be directly measured from the absorption spectra of the thermodynamically stable *trans* stereoisomer, and considering that ε_{CH} and ε_{C} can be roughly estimated (see ref. [44] and Figure 2S in the Supporting Information), $\Phi_{TH\rightarrow CH}$, $\Phi_{CH\rightarrow TH}$, $\Phi_{C\rightarrow T}$, and $\Phi_{T\rightarrow C}$ can be additionally extracted. For TH_2Cl_3 at 347 nm, we found $\varepsilon_{TH}(347)\Phi_{TH\rightarrow CH}(347) = 630\,M^{-1}cm^{-1}$, $\varepsilon_{CH}(347)\ \Phi_{CH\rightarrow TH}(347) = 140\,M^{-1}cm^{-1}$, $\varepsilon_{C}(347)\ \Phi_{C\rightarrow T}(347) = 260\,M^{-1}cm^{-1}$, $\varepsilon_{T}(347)\Phi_{T\rightarrow C}(347) \approx 290\,M^{-1}cm^{-1}$;[50] from which we subsequently derived $\Phi_{TH\rightarrow CH}(347) = 3\,\%$, $\Phi_{CH\rightarrow TH}(347) \approx 2\,\%$, $\Phi_{C\rightarrow T}(347) \approx 18\,\%$, and $\Phi_{T\rightarrow C}(347) \approx 6\,\%$ by using $\varepsilon_{TH}(347) = 2\times10^{4}\,M^{-1}cm^{-1}$, $\varepsilon_{CH}(347) \approx 6\times10^{3}\,M^{-1}cm^{-1}$, $\varepsilon_{C}(347) \approx 1.4\times10^{3}\,M^{-1}cm^{-1}$, and $\varepsilon_{T}(347) = 4.8\times10^{3}\,M^{-1}cm^{-1}$.

Pulses and oscillations of proton concentration: Equipped with the preceding derivation of thermodynamic and kinetic constants, we were able to devise a series of experiments aimed at observing both pulses and oscillations of proton concentration. We submitted degassed solutions of 2-hydroxyazobenzene in water/acetonitrile 1:1 (v/v) to various sequences of illumination. The photogenerated variations of proton concentration were detected by two different means. We first relied on a glass electrode by observing light-induced drops of the pH-meter indication. We also used a fluorescent reporter of the proton concentration to facilitate the measurements by relying on optical detection only.

Pulses of proton concentration: Our glass electrode was not sensitive to UV light in the range of investigated powers: We observed no response to illumination in water/acetonitrile 1:1 (v/v). In contrast, we observed up to 2 pH-unit drops in solutions that contained either TH_2Cl_3 or $THSO_3KCl_3$ at 200–300 μM concentration (Figure 2a) when they were submitted to a strong UV illumination. As expected from the photogeneration of the more acidic *cis* stereoisomer in the presence of UV light, the proton concentration increases and then stabilizes when the steady state is reached. In contrast, turning off the light results in the relaxation of the proton concentration to the initial unilluminated state. The relaxation timescale is about ten times faster for $THSO_3KCl_3$ than for TH_2Cl_3, as expected from a consideration of the increasing value of the thermal *cis*-to-*trans* isomerization rate constant when the substituent group R is more and more electron-withdrawing.

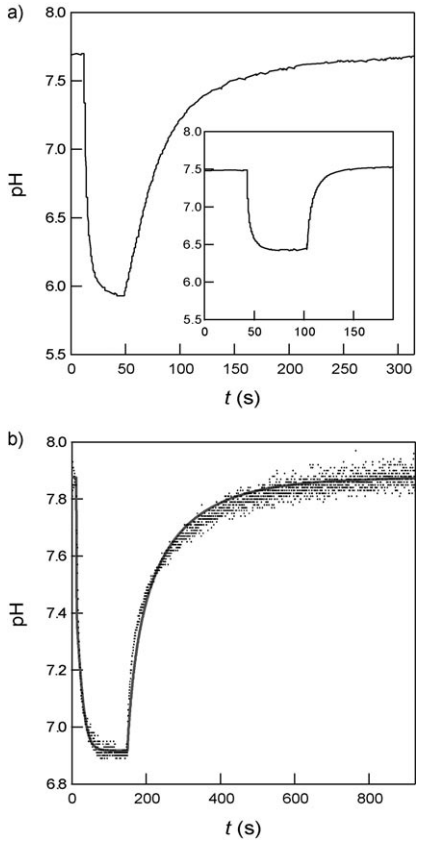

Figure 2. Proton concentration pulses upon transient illumination a) as measured with the pH meter in 6 mL of 220 μM TH_2Cl_3 (or 330 μM $THSO_3KCl_3$; inset) submitted to a 30 s-long (respectively, 50) 365 nm pulse delivering 1.2×10^{-5} Einstein s^{-1} (with a flux of 1.7×10^{-6} Einstein $s^{-1}cm^{-2}$) at the sample; b) as measured with the fluorescein reporter in 105 μM TH_2Cl_3 (2 mL), 10 nM rhodamine B, and 10 nM fluorescein submitted to a 150 s-long pulse delivering 1.9×10^{-7} Einstein s^{-1} (with a flux of 1.9×10^{-7} Einsteins^{-1} cm^{-2}) at the sample. Solid line: Fit resulting from numerical simulations (see the Supporting Information). Solvent: degassed water/acetonitrile 1:1 (v/v). $T = 298$ K.

To circumvent any limitation associated with the one- to ten-second response time of the glass electrode, we alternatively relied on a fluorescent reporter, which can be used down to the millisecond timescale to analyze the temporal variations of proton concentration. Considering the investigated pH range, we chose fluorescein, which exhibits $pK_{Flu}=7.6$ in the considered solvent. Since fluorescein emission depends not only on proton concentration but also on the intensity of the exciting source, we also added the pH-insensitive rhodamine B to report on the variation of the sample absorbance associated with the *trans*-to-*cis* isomerization of the 2-hydroxyazobenzenes (see above). Therefore the ratio of the fluorescence emission from fluorescein and from rhodamine B gives access to the desired proton concentration after calibration (see Figures 9S and 10S in the Supporting Information). Figure 2b displays the typical pH drop observed upon submitting around 100 μM TH_2Cl_3 to a 365 nm pulse generated with the fluorometer light source. As anticipated from the lower illumination power and the lower TH_2Cl_3 concentration, the pH drop in Figure 2b is smaller than the one in Figure 2a.

The preceding pH drops have been evaluated for their consistency with the thermodynamic, kinetic, and photochemical properties evaluated above. Taking into account all the chemical reactions of the system, the temporal evolution of the chemical concentrations was simulated using the known set of parameters and the experimental curves were fitted by adjusting the remaining parameters (see Supporting Information). Starting from the simulation of the behavior observed by using fluorescein to report on pH, we obtained a satisfactory fit of the experimental data (see Figure 2b) by considering that the illuminated solution contained a minor (70 μM) weak base contaminant. It was suggested that it was made of residual carbonates from analyzing ionization constants as well as the rate constant associated with an acidic state decomposition that we attributed to H_2CO_3 (see the Supporting Information). In particular, the resulting set of fitting parameters was also appropriate for fitting the amplitude of the photogenerated pH change displayed in Figure 2a. Thus the numerical simulations showed that the observed pH drops were consistent with all the kinetic and thermodynamic parameters experimentally determined in the present work or available in the literature. However, they also suggested that, as anticipated, the presence of buffering species (here residual carbonates) may dampen the photogenerated pH drop from illuminating 2-hydroxybenzene derivatives.

Oscillations of proton concentration: After generating pulses of proton concentration, we were interested in evaluating whether modulations of the UV light source can lead to the modulation of pH. For this series of experiments, we retained the highly soluble $THSO_3KCl_3$ 2-hydroxyazobenzene. Indeed, this derivative was expected to exhibit one of the fastest thermal returns of its *cis* stereoisomer, thereby allowing us to perform significant pH modulation at the highest frequencies. The pH values and proton concentrations have been deduced from analysis of the fluorescence variations of fluorescein and rhodamine B as described above and in the Supporting Information (see Figure 11S).

We first explored conditions of weak illumination modulation to remain in the regime of first-order perturbation theoretically calculated in the Supporting Information (Figure 3a). As predicted, the proton concentration exhibits a sinusoidal modulation at the excitation frequency: for a 40% 210 mHz modulation of the 365 nm UV light around the 7.2×10^{-8} Einstein s^{-1} average value, we observed a 11% modulation of the proton concentration delayed by $\phi=0.4$ rad with regard to light modulation. Using Equation (23) in the Supporting Information, we retrieved from the preceding observations the sum of the rate constants associated with the *trans*-to-*cis* and *cis*-to-*trans* $THSO_3KCl_3$ isomerizations: $k^{h\nu}_{TH\rightarrow C}+k^{h\nu}_{C\rightarrow TH}+k^{\Delta}_{C\rightarrow TH}=0.5\ s^{-1}$. This estimate is in line with the corresponding value that can be directly extracted

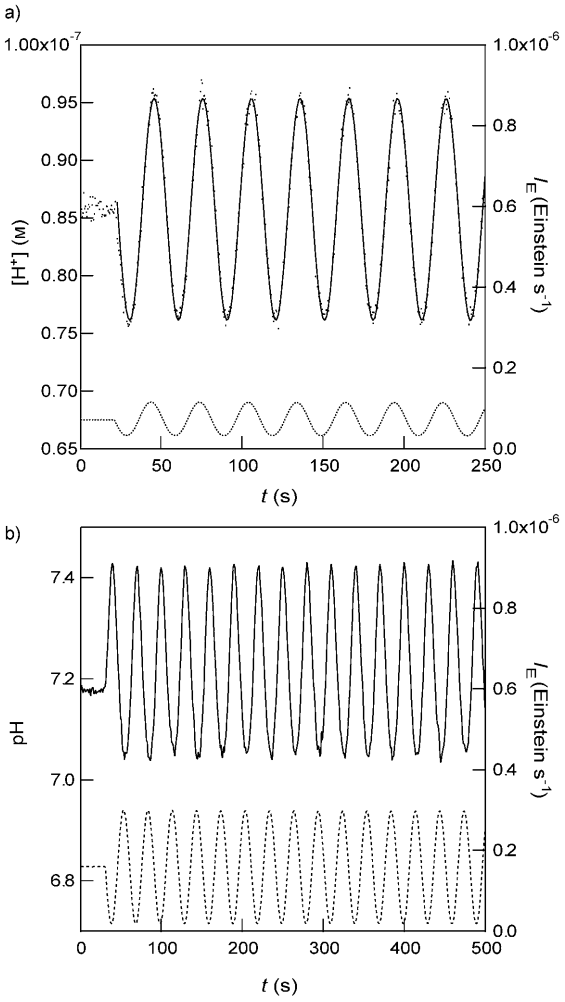

Figure 3. Oscillations of proton concentration (solid line) as measured with the fluorescein reporter upon applying a periodic sinusoidal modulation of the UV illumination (dotted line), $I_E=(I_E)(1+\beta\sin\omega t)$, to a solution that contained 300 μM $THSO_3KCl_3$, 10 nM rhodamine B, and 10 nM fluorescein. a) $I_E=7.2\times10^{-8}$ Einstein s^{-1}, $\beta=0.4$, and $\omega=210$ mHz; b) $I_E=1.6\times10^{-7}$ Einstein s^{-1}, $\beta=0.9$, and $\omega=210$ mHz. Solvent: degassed water/acetonitrile 1:1 (v/v). $T=298$ K.

from the timescale for $THSO_3KCl_3$ photoisomerization: With Equation (51) in the Supporting Information and the data shown in the inset of Figure 2a, we derived: $k^{h\nu}_{TH\rightarrow C}+k^{h\nu}_{C\rightarrow TH}+k^{\Delta}_{C\rightarrow TH}=0.3\ s^{-1}$.

Figure 3b shows that much larger pH modulations can be obtained upon applying larger sinusoidal modulations of the UV light intensity: In a degassed 300 μM $THSO_3KCl_3$ solution, pH periodically varied between 7.0 and 7.4 when the light intensity was sinusoidally modulated at 210 mHz by 90% around the average value of 1.6×10^{-7} Einstein s^{-1} (see also Figure 11S in the Supporting Information). Moreover, other periodical patterns can be applied to the sample. As an example, Figure 12S displays the pH evolution that can be obtained from applying a triangular periodical illumination.

Conclusion

This study demonstrates that the 2-hydroxyazobenzene series provides a versatile platform for the design of reversible photoacids to generate significant pH pulses and oscillations with monochromatic light. The syntheses are easy and numerous synthons will be available to tune solubility as well as to graft the 2-hydroxyazobenzene moiety onto various molecular backbones. The photoisomerization behavior associated with phenol ionization is robust and capable of photoincreasing proton concentration by typically two orders of magnitude in neutral media. The Gibbs free-energy relationships we derived for the protonation constants of the *trans* and *cis* stereoisomers as well as for the rate constant for thermal *cis*-to-*trans* isomerization of 2-hydroxyazobenzenes make it possible to predict which substitution patterns at the phenyl and phenol rings should be chosen to observe a given amplitude of pH change under specific illumination conditions. In particular, we showed that analytic calculations and numerical simulations satisfactorily accounted for our results.

In addition to the preceding remarks that focus on the photogeneration of protons, this study can also be seen as providing a generic photochromic unit, the charge of which will change upon illumination in a wide pH range around neutrality. Considering the wide use of the azobenzene moiety as a photoswitch, this alternative perspective should attract attention given the major structural change that occurs upon illumination of the 2-hydroxyazobenzene backbone.

Experimental Section

Reagents and solutions: Fluorescein, rhodamine B, and acetonitrile were purchased from Sigma–Aldrich, TCI Europe, and Fischer Scientific. Hydrochloric acid (5 M) was prepared from a commercial 37% solution. Sodium hydroxide solution (9.2 M) was commercially available. All solutions were prepared with water purified using a Direct-Q 5 instrument (Millipore, Billerica, MA). The Britton–Robinson buffers were prepared according to Frugoni.[39] The water/acetonitrile solutions were degassed either by bubbling N_2 for 10 min (when the pH meter was used to report on pH pulses) or by freeze–thaw cycling three times under vacuum (when fluorescence was used to report on pH pulses and oscillations).

pH measurements: By assimilating activity and concentration, the proton concentration in acetonitrile/water 1:1 (v/v) solutions was directly measured after calibration of the pH meter (Standard pH meter PHM210, Radiometer Analytical equipped with Radiometer Analytical electrodes) with various buffers (acetic acid, phosphoric acid, and boric acid; 50 mM concentration in both the acidic and the basic states), for which the ionization constants in acetonitrile/water 1:1 (v/v) solutions have been reported.[51–53]

UV/Vis absorption and steady-state emission spectroscopies: UV/Vis absorption spectra were recorded using a Uvikon-940 spectrophotometer (Kontron, Zürich, Switzerland). Corrected fluorescence spectra were acquired using a LPS 220 spectrofluorometer (PTI, Monmouth Junction, NJ). The quartz cuvettes (Hellma) were 1×1 cm. The temperature of the holders was maintained by using a thermostat of circulating baths (Polystat 34-R2, Fisher Bioblock Scientific, Illkirch, France), and the temperature was directly measured in the cuvettes using a type K thermocouple connected to a ST-610B digital pyrometer (Stafford Instruments, Stafford, UK).

Stopped-flow experiments were performed using a RX2000 rapid kinetic stopped-flow accessory (Applied Photophysics, Leatherhead, UK) adapted to the LPS 220 spectrofluorometer. In this setup, two 100 μL solutions were mixed with typical dead times of 100 ms and the fluorescence intensity was recorded over time at 3 Hz.

Irradiation experiments: Different protocols have been used to perform the irradiations.

Protocol 1: For the preliminary experiment to evidence the *trans*-to-*cis* photoisomerization of TH_2Cl_3 (Figure 2S in the Supporting Information), we put a bench-top UV lamp (6 W, 365 nm UV lamp; Fisher Bioblock) above a 1×1 cm quartz cuvette that contained the solution (2 mL) that was subsequently transferred into the UV/Vis spectrometer.

Protocol 2: The experiments to acquire the photochemical properties of the investigated 2-hydroxyazobenzenes were performed using the stopped-flow apparatus (RX.2000 Stopped-Flow Mixing Accessory, Applied Photophysics) upon illuminating the contents of the 1×0.2 cm quartz cuvette (≈200 μL) with the 75 W xenon lamp of the Photon Technology International LPS 220 spectrofluorometer at several slit widths to cover a significant range of incident light intensities.

Protocol 3: The experiments devoted to the generation of pH pulses and oscillations were performed by following two protocols. 1) When the pH variation was reported by a pH meter, the experiment was done on samples (6 mL) in a small beaker submitted to a pulse of light from a Hamamatsu LC8L9588 UV lamp. 2) When the pH variation was followed by fluorescence spectroscopy, the experiment was done on samples (2 mL) in 1×1 cm quartz cuvettes continuously subjected to a weak illumination at 500 nm and additionally subjected to either pulse or periodic oscillations of the light from a UV-emitting diode (Nichia chip UV LED NCSU033A(T), 0–700 mA), either by turning the on/off cycle or by using an Agilent 33220A, 20 MHz function, arbitrary waveform generator.

In all cases, the incident-light intensities were calibrated by determining the kinetics of photoconversion of the α-(4-dimethylaminophenyl)-*N*-phenylnitrone into 3-(4-dimethylaminophenyl)-2-phenyloxaziridine in absolute ethanol as described in ref. [54]. During the present series of experiments, the typical photon flux at the sample was in the 10^{-5}–10^{-10} Einstein s^{-1} range.

Data processing: The evolutions of the TH absorbance as a function of pH were analyzed using the SPECFIT/32 Global Analysis System (Version 3.0 for 32-bit Windows systems) to extract their p*K*.[55] The other data have been processed and fitted with Igor Pro 6 (WaveMetrics, Lake Oswego, OR).

Computer simulation: Simultaneously computing very slow and very fast chemical reactions as in the present system requires an algorithm capable of dealing with such a "stiff" set of ordinary differential equations (ODE). Classical all-purpose algorithms (for instance, the Runge–Kutta methods) would lead the simulation to scale on the fastest reactions, and

thus advance the computation by very small time steps, even when it is not necessary.[56] The time evolution was thus computed using an implicit method, the Bulirsch–Stoer algorithm.[57] For each run with a given set of normalized parameters p, it was possible to evaluate the distance $\delta(\boldsymbol{p})$ between the simulated evolution $pH_{sim}(\boldsymbol{p},t)$ with the experimental data $pH_{exp}(\boldsymbol{p},t)$ by using Equation (1), for all the experimental values of t, taken at regular time intervals:

$$\delta(\boldsymbol{p}) = \sum_{t=0}^{t_{end}} [pH_{sim}(\boldsymbol{p},t) - pH_{exp}(\boldsymbol{p},t)]^2 \quad (1)$$

To automatically adjust some parameters to fit the experimental curve, the function $\delta(\boldsymbol{p})$ was minimized using a simplex algorithm.[58]

The simulation program was implemented in C (GCC, GNU Scientific Library) using the Burlisch–Stoer algorithm for the ODE numerical integration and the simplex algorithm for the parameter optimization available in the Gnu Scientific Library (GSL).[59] Fully documented source code is available as Supporting Information (see file phjump.c). The simulations were computed using a Lenovo R61 laptop, with an Intel Core2-Duo Mobile Processor T7250. One typical simulation run takes a couple of seconds of computation, and one parameter optimization process takes a couple of minutes.

Acknowledgements

We are thankful to Axel Brandenburg for useful discussions. We also thank for their support Nordita (concerning the computer simulations), the Pierre-Gilles de Gennes Foundation (for a grant) and the European program COST "System Chemistry" CM0703 (for its support).

[1] M. Eigen, *Angew. Chem.* **1963**, *75*, 489–508; *Angew. Chem. Int. Ed. Engl.* **1964**, *3*, 1–19.
[2] W. P. Jencks, *Catalysis in Chemistry and Enzymology*, Dover Publications, New York, **1987**.
[3] R. N. Goldberg, N. Kishore, R. M. Lennen, *J. Phys. Chem. Ref. Data* **2002**, *31*, 231–370.
[4] S. Khan, F. Castellano, J. L. Spudich, J. A. McCray, R. S. Goody, G. P. Reid, D. R. Trentham, *Biophys. J.* **1993**, *65*, 2368–2382.
[5] A. Barth, J. E. T. Corrie, *Biophys. J.* **2002**, *83*, 2864–2871.
[6] M. V. Georges, J. C. Scaiano, *J. Phys. Chem.* **1980**, *84*, 492–495.
[7] K. Janko, J. Reichert, *Biochim. Biophys. Acta* **1987**, *905*, 409–416.
[8] G. Bonetti, A. Vecli, C. Viappiani, *Chem. Phys. Lett.* **1997**, *269*, 268–273.
[9] For a system capable of photodelivering pulses of the hydroxide anion, see: M. Irie, *J. Am. Chem. Soc.* **1983**, *105*, 2078–2079.
[10] M. Eigen, L. de Mayer, *Relaxation Methods in Techniques of Organic Chemistry, Vol. VIII*, 2nd ed. (Eds.: S. L. Friess, E. S. Lewis, A. Weissberger) Wiley, New York, **1963**, pp. 895–1054.
[11] D. Baurecht, U. P. Fringeli, *Rev. Sci. Instrum.* **2001**, *72*, 3782–3792.
[12] K. Kurin-Csörgei, I. R. Epstein, M. Orbán, *Nature* **2005**, *433*, 139–142.
[13] D. Liu, S. Balasubramanian, *Angew. Chem.* **2003**, *115*, 5912–5914; *Angew. Chem. Int. Ed.* **2003**, *42*, 5734–5736.
[14] T. Liedl, F. C. Simmel, *Nano Lett.* **2005**, *5*, 1894–1898.
[15] J. R. Howse, P. Topham, C. J. Crook, A. J. Gleeson, W. Bras, R. A. L. Jones, A. J. Ryan, *Nano Lett.* **2006**, *6*, 73–77.
[16] M. Gutman, D. Huppert, E. Pines, *J. Am. Chem. Soc.* **1981**, *103*, 3709–3713.
[17] L. M. Tolbert, K. M. Solntsev, *Acc. Chem. Res.* **2002**, *35*, 19–27.
[18] U. Steiner, M. H. Abdel-Kader, P. Fischer, H. E. A. Kramer, *J. Am. Chem. Soc.* **1978**, *100*, 3190–3197.
[19] S. H. Kawai, S. L. Gilat, J.-M. Lehn, *Eur. J. Org. Chem.* **1999**, 2359–2366.
[20] Y. Odo, K. Matsuda, M. Irie, *Chem. Eur. J.* **2006**, *12*, 4283–4288.
[21] G. Wettermark, *J. Phys. Chem.* **1962**, *66*, 2560–2562.
[22] R. Haag, J. Wirz, P. J. Wagner, *Helv. Chim. Acta* **1977**, *60*, 2595–2607.
[23] Y. Eichen, J.-M. Lehn, M. Scherl, D. Haarer, R. Casalegno, A. Corval, K. Kuldovac, H. P. Trommsdorff, *J. Chem. Soc. Chem. Commun.* **1995**, 713–714.
[24] For a report that illustrates the lack of robustness of a closely related photochemistry by shifting the maximum wavelength absorption to the red, see: I. Aujard, C. Benbrahim, M. Gouget, O. Ruel, J.-B. Baudin, P. Neveu, L. Jullien, *Chem. Eur. J.* **2006**, *12*, 6865–6879.
[25] L. Jullien, A. Lemarchand, S. Charier, O. Ruel, J.-B. Baudin, *J. Phys. Chem. B* **2003**, *107*, 9905–9917.
[26] T. Matsuhira, K. Tsuchihashi, H. Yamamoto, T. Okamura, N. Ueyama, *Org. Biomol. Chem.* **2008**, *6*, 3118–3126.
[27] R. S. Stoll, M. V. Peters, A. Kuhn, S. Heiles, R. Goddard, M. Bühl, C. M. Thiele, S. Hecht, *J. Am. Chem. Soc.* **2009**, *131*, 357–367.
[28] P. Haberfield, *J. Am. Chem. Soc.* **1987**, *109*, 6177–6178.
[29] G. Wettermark, M. E. Langmuir, D. G. Anderson, *J. Am. Chem. Soc.* **1965**, *87*, 476–481.
[30] E. Fischer, Y. F. Frei, *J. Chem. Soc.* **1959**, 3159–3163.
[31] G. Gabor, E. Fischer, *J. Phys. Chem.* **1962**, *66*, 2478–2481.
[32] J. Griffiths, *Chem. Soc. Rev.* **1972**, *1*, 481–493.
[33] S. Kobatake, M. Irie, *Annu. Rep. Prog. Chem. Sect. C* **2003**, *99*, 277–313.
[34] G. Mayer, A. Heckel, *Angew. Chem.* **2006**, *118*, 5020–5042; *Angew. Chem. Int. Ed.* **2006**, *45*, 4900–4921.
[35] H. T. Clarke, W. R. Kirner, *Org. Synth. Coll. Vol.* **1941**, *1*, 374–377.
[36] A. Vogel, *Textbook of Practical Organic Chemistry*, 4th ed., Longman, München, **1978**, pp. 714–715.
[37] S. Darwish, H. M. Fahmy, M. A. Abdel Aziz, A. A. Et Maghraby, *J. Chem. Soc. Perkin Trans. 2* **1981**, 344–349.
[38] T. Kunitake, Y. Okahata, M. Shimomura, S. Yasunami, K. Takarabe, *J. Am. Chem. Soc.* **1981**, *103*, 5401–5413.
[39] C. Frugoni, *Gazz. Chim. Ital.* **1957**, *87*, 403–407.
[40] H. H. Jaffé, *Chem. Rev.* **1953**, *53*, 191–261.
[41] C. A. Reichardt, *Solvents and Solvent Effects in Organic Chemistry*, 3rd ed., VCH, Weinheim, **2003**.
[42] M. B. Smith, J. March, *Advanced Organic Chemistry*, 5th ed., Wiley Interscience, New York, **2001**.
[43] The negative slope is also in agreement with an increase of the stabilization of the conjugate base $TRCl_3$ when R becomes more and more electron withdrawing. However the slope value that is larger than 1 suggests that the position subjected to the R influence is close to the substituted phenyl ring.
[44] G. Gabor, Y. Frei, D. Gegiou, M. Kaganowitch, E. Fischer, *Isr. J. Chem.* **1967**, *7*, 193–221.
[45] H. Rau, *Photochromism: Molecules and Systems* (Eds.: H. Dürr, H. Bouas-Laurent), Elsevier, Amsterdam, **1990**.
[46] D. Stefanidis, S. Cho, S. Dhe-Paganon, W. P. Jencks, *J. Am. Chem. Soc.* **1993**, *115*, 1650–1656.
[47] N. Gagey, P. Neveu, C. Benbrahim, B. Goetz, I. Aujard, J.-B. Baudin, L. Jullien, *J. Am. Chem. Soc.* **2007**, *129*, 9986–9998.
[48] N. Gagey, P. Neveu, L. Jullien, *Angew. Chem.* **2007**, *119*, 2519–2521; *Angew. Chem. Int. Ed.* **2007**, *46*, 2467–2469.
[49] N. Gagey, M. Emond, P. Neveu, C. Benbrahim, B. Goetz, I. Aujard, J.-B. Baudin, L. Jullien, *Org. Lett.* **2008**, *10*, 2341–2344.
[50] It was not possible to directly retrieve an accurate value for $\varepsilon_T(347)\Phi_{T\rightarrow C}(347)$ from the preceding data treatment. We were only able to derive an upper limit equal to $500\,M^{-1}cm^{-1}$ (see Figure 8S in the Supporting Information). In fact, we used the relative proportions in C and T obtained by NMR spectroscopy (see Figure 3S) and the more precisely derived value of $\varepsilon_C(347)\Phi_{C\rightarrow T}(347)$ to get a more precise value of $\varepsilon_T(347)\Phi_{T\rightarrow C}(347)$.
[51] S. Espinosa, E. Bosch, M. Rosés, *Anal. Chem.* **2000**, *72*, 5193–5200.
[52] J. Barbosa, V. Sanz-Nebot, *J. Pharm. Biomed. Anal.* **1992**, *10*, 1047–1051.
[53] J. Barbosa, V. Sanz-Nebot, *Anal. Chim. Acta* **1991**, *244*, 183–191.
[54] P. F. Wang, L. Jullien, B. Valeur, J.-S. Filhol, J. Canceill, J.-M. Lehn, *New J. Chem.* **1996**, *20*, 895–907.

[55] H. Gampp, M. Maeder, C. J. Meyer, A. D. Zuberbühler, *Talanta* **1985**, *32*, 95–101; H. Gampp, M. Maeder, C. J. Meyer, A. D. Zuberbühler, *Talanta* **1985**, *32*, 257–264; H. Gampp, M. Maeder, C. J. Meyer, A. D. Zuberbühler, *Talanta* **1985**, *32*, 1133–1139; H. Gampp, M. Maeder, C. J. Meyer, A. D. Zuberbühler, *Talanta* **1986**, *33*, 943–951.

[56] W. H. Press, S. A. Teukolsky, W. T. Vetterling, B. P. Flannery, *Numerical Recipes in C: The Art of Scientific Computing*, 2nd ed., Cambridge University Press, New York, **1992**.

[57] G. Bader, P. Deuflhard, *Numer. Math.* **1983**, *41*, 373–398.

[58] J. A. Nelder, R. Mead, *Comput. J.* **1965**, *7*, 308–313.

[59] Gnu Scientific Library, http://www.gnu.org/software/gsl/.

Received: March 2, 2010
Published online: June 25, 2010

